

Mobile Robot Positioning – Sensors and Techniques

by

J. Borenstein¹, H.R. Everett², L. Feng³, and D. Wehe⁴

ABSTRACT

Exact knowledge of the position of a vehicle is a fundamental problem in mobile robot applications. In search for a solution, researchers and engineers have developed a variety of systems, sensors, and techniques for mobile robot positioning. This paper provides a review of relevant mobile robot positioning technologies. The paper defines seven categories for positioning systems: 1. Odometry; 2. Inertial Navigation; 3. Magnetic Compasses; 4. Active Beacons; 5. Global Positioning Systems; 6. Landmark Navigation; and 7. Model Matching. The characteristics of each category are discussed and examples of existing technologies are given for each category.

The field of mobile robot navigation is active and vibrant, with more great systems and ideas being developed continuously. For this reason the examples presented in this paper serve only to represent their respective categories, but they do not represent a judgment by the authors. Many ingenious approaches can be found in the literature, although, for reasons of brevity, not all could be cited in this paper.

¹⁾ (Corresponding Author) The University of Michigan, Advanced Technologies Lab, 1101 Beal Avenue, Ann Arbor, MI 48109-2110, Ph.: 313-763-1560, Fax: 313-944-1113. Email: johannb@umich.edu

²⁾ Naval Command, Control, and Ocean Surveillance Center, RDT&E Division 5303, 271 Catalina Boulevard, San Diego, CA 92152-5001, Email: Everett@NOSC.MIL

³⁾ The University of Michigan, Advanced Technologies Lab, 1101 Beal Avenue, Ann Arbor, MI 48109-2110, Email: Feng@engin.umich.edu

⁴⁾ The University of Michigan, Dept. of Nuclear Engineering and Radiological Sciences, 239 Cooley Bldg., Ann Arbor, MI 48109, Email: dkw@umich.edu

Report Documentation Page

*Form Approved
OMB No. 0704-0188*

Public reporting burden for the collection of information is estimated to average 1 hour per response, including the time for reviewing instructions, searching existing data sources, gathering and maintaining the data needed, and completing and reviewing the collection of information. Send comments regarding this burden estimate or any other aspect of this collection of information, including suggestions for reducing this burden, to Washington Headquarters Services, Directorate for Information Operations and Reports, 1215 Jefferson Davis Highway, Suite 1204, Arlington VA 22202-4302. Respondents should be aware that notwithstanding any other provision of law, no person shall be subject to a penalty for failing to comply with a collection of information if it does not display a currently valid OMB control number.

1. REPORT DATE 1997	2. REPORT TYPE N/A	3. DATES COVERED -			
4. TITLE AND SUBTITLE Mobile Robot Positioning - Sensors and Techniques					
5a. CONTRACT NUMBER 					
5b. GRANT NUMBER 					
5c. PROGRAM ELEMENT NUMBER 					
6. AUTHOR(S) 					
5d. PROJECT NUMBER 					
5e. TASK NUMBER 					
5f. WORK UNIT NUMBER 					
7. PERFORMING ORGANIZATION NAME(S) AND ADDRESS(ES) RDT&E Division, Naval Command, Control and Ocean Surveillance Center San Diego, CA 92152-7383					
8. PERFORMING ORGANIZATION REPORT NUMBER 					
9. SPONSORING/MONITORING AGENCY NAME(S) AND ADDRESS(ES) 					
10. SPONSOR/MONITOR'S ACRONYM(S) 					
11. SPONSOR/MONITOR'S REPORT NUMBER(S) 					
12. DISTRIBUTION/AVAILABILITY STATEMENT Approved for public release, distribution unlimited					
13. SUPPLEMENTARY NOTES The original document contains color images.					
14. ABSTRACT 					
15. SUBJECT TERMS 					
16. SECURITY CLASSIFICATION OF: <table border="1" style="width: 100%; border-collapse: collapse;"> <tr> <td style="width: 33%;">a. REPORT unclassified</td> <td style="width: 33%;">b. ABSTRACT unclassified</td> <td style="width: 34%;">c. THIS PAGE unclassified</td> </tr> </table>			a. REPORT unclassified	b. ABSTRACT unclassified	c. THIS PAGE unclassified
a. REPORT unclassified	b. ABSTRACT unclassified	c. THIS PAGE unclassified			
17. LIMITATION OF ABSTRACT UU	18. NUMBER OF PAGES 23	19a. NAME OF RESPONSIBLE PERSON 			

1. INTRODUCTION

This paper surveys the state-of-the-art in sensors, systems, methods, and technologies that aim at finding a mobile robot's position in its environment. In surveying the literature on this subject, it became evident that a benchmark-like comparison of different approaches is difficult because of the lack of commonly accepted test standards and procedures. The research platforms used differ greatly and so do the key assumptions used in different approaches. Further challenges arise from the fact that different systems are at different stages in their development. For example, one system may be commercially available, while another system, perhaps with better performance, has been tested only under a limited set of laboratory conditions. For these reasons we generally refrain from comparing or even judging the performance of different systems or techniques. Furthermore, we have not tested most of the systems and techniques, so the results and specifications given in this paper are derived from the literature. Finally, we should point out that a large body of literature related to navigation of aircraft, space craft, or even artillery addresses some of the problems found in mobile robot navigation (e.g., [Farrell, 1976; Battin, 1987]. However, we have focused our survey only on literature pertaining directly to mobile robots. This is because sensor systems for mobile robots must usually be relatively small, lightweight, and inexpensive. Similarly we are not considering Automated Guided Vehicles (AGVs) in this article. AGVs use magnetic tape, buried guide wires, or painted stripes on the ground for guidance. These vehicles are thus not freely programmable and they cannot alter their path in response to external sensory input (e.g., obstacle avoidance). However, the interested reader may find a survey of guidance techniques for AGVs in [Everett, 1995].

Perhaps the most important result from surveying the literature on mobile robot positioning is that, to date, there is no truly elegant solution for the problem. The many partial solutions can roughly be categorized into two groups: relative and absolute position measurements. Because of the lack of a single good method, developers of mobile robots usually combine two methods, one from each group. The two groups can be further divided into the following seven categories:

- I: Relative Position Measurements (also called Dead-reckoning)
 - 1. Odometry
 - 2. Inertial Navigation
- II: Absolute Position Measurements (Reference-based systems)
 - 3. Magnetic Compasses
 - 4. Active Beacons
 - 5. Global Positioning Systems
 - 6. Landmark Navigation
 - 7. Model Matching

2. REVIEW OF SENSORS AND TECHNIQUES

In this Section we will review some of the sensors and techniques used in mobile robot positioning. Examples of commercially available systems or well-documented research results will also be given.

2.1 Odometry

Odometry is the most widely used navigation method for mobile robot positioning; it provides good short-term accuracy, is inexpensive, and allows very high sampling rates. However, the fundamental idea of odometry is the integration of incremental motion information over time, which leads inevitably to the unbounded accumulation of errors. Specifically, orientation errors will cause large lateral position errors, which increase proportionally with the distance traveled by the robot. Despite these limitations, most researchers agree that odometry is an important part of a robot navigation system and that navigation tasks will be simplified if odometric accuracy can be improved. For example Cox [1991], Byrne et al. [1992], and Chenavier and Crowley [1992], propose methods for fusing odometric data with absolute position measurements to obtain more reliable position estimation.

Odometry is based on simple equations (see [Borenstein et al., 1996a]), which hold true when wheel revolutions can be translated accurately into linear displacement relative to the floor. However, in case of wheel slippage and some other more subtle causes, wheel rotations may not translate proportionally into linear motion. The resulting errors can be categorized into one of two groups: *systematic errors* and *non-systematic errors* [Borenstein and Feng, 1996]. Systematic errors are those resulting from kinematic imperfections of the robot, for example, unequal wheel diameters or uncertainty about the exact wheelbase. Non-systematic errors are those that result from the interaction of the floor with the wheels, e.g., wheel slippage or bumps and cracks. Typically, when a mobile robot system is installed with a hybrid odometry/landmark navigation system, the density in which the landmarks must be placed in the environment is determined empirically and is based on the worst-case systematic errors. Such systems are likely to fail when one or more large non-systematic errors occur.

2.1.1 Measurement of Odometry Errors

One important but rarely addressed difficulty in mobile robotics is the *quantitative* measurement of odometry errors. Lack of well-defined measuring procedures for the quantification of odometry errors results in the poor calibration of mobile platforms and incomparable reports on odometric accuracy in scientific communications. To overcome this problem Borenstein and Feng [1995] developed a method for quantitatively measuring systematic odometry errors and, to a limited degree, non-systematic odometry errors. This method, called *University of Michigan Benchmark* (UMBmark) requires that the mobile robot be programmed to follow a pre-programmed square path of 4×4 m side-length and four on-the-spot 90-degree turns. This run is to be performed five times in clockwise (cw) and five times in counter-clockwise (ccw) direction.

When the return position of the robot as computed by odometry is compared to the actual return position, an error plot similar to the one shown in Figure 1 will result. The results of Figure 1 can be interpreted as follows:

- The stopping positions after cw and ccw runs are clustered in two distinct areas.
- The distribution within the cw and ccw clusters are the result of non-systematic errors. However, Figure 1 shows that in an uncalibrated vehicle, traveling over a reasonably smooth concrete floor, the contribution of *systematic* errors to the total odometry error can be nota-

bly larger than the contribution of non-systematic errors.

The asymmetry of the centers of gravity in cw and ccw results from the dominance of two types of systematic errors, collectively called Type A and Type B [Borenstein and Feng, 1996]. Type A errors are defined as orientation errors that reduce (or increase) the amount of rotation of the robot during the square path experiment in *both* cw and ccw direction. By contrast, Type B errors reduce (or increase) the amount of rotation when traveling in cw but have the opposite effect when traveling in ccw direction. One typical source for Type A errors is the uncertainty about the effective wheelbase; a typical source for Type B errors is unequal wheel diameters.

After conducting the UMBmark experiment a single numeric value that expresses the odometric accuracy (with respect to systematic errors) of the tested vehicle can be found from [Borenstein and Feng, 1996]:

$$E_{\max,\text{syst}} = \max(r_{c.g.,\text{cw}}; r_{c.g.,\text{ccw}}). \quad (1)$$

where

$$r_{c.g.,\text{cw}} = \sqrt{(x_{c.g.,\text{cw}})^2 + (y_{c.g.,\text{cw}})^2}$$

and

$$r_{c.g.,\text{ccw}} = \sqrt{(x_{c.g.,\text{ccw}})^2 + (y_{c.g.,\text{ccw}})^2}.$$

Based on the UMBmark test, Borenstein and Feng [1995; 1996] developed a calibration procedure for reducing systematic odometry errors in differential drive vehicles. In this procedure the UMBmark test is performed five times in cw and ccw direction to find $x_{c.g.,\text{cw}}$ and $x_{c.g.,\text{ccw}}$. From a set of equations defined in [Borenstein and Feng, 1995; 1996] two calibration constants are found that can be included in the basic odometry computation of the robot. Application of this procedure to several differential-drive platforms resulted consistently in a 10- to 20-fold reduction in systematic errors. Figure 2 shows the result of a typical calibration session. $E_{\max,\text{syst}}$ The results for many runs calibration sessions with TRC's LabMate robots averaged $E_{\max,\text{syst}} = 330$ mm for uncalibrated vehicles and $E_{\max,\text{syst}} = 24$ mm after calibration.

2.1.2 Measurement of Non-Systematic Errors

Borenstein and Feng [1995] also proposes a method for measuring non-systematic errors. This method, called *extended UMBmark*, can be used for comparison of different robots under similar conditions, although the measurement of non-systematic errors is less useful because it depends strongly on the floor characteristics. However, using a set of well-defined floor irregularities and

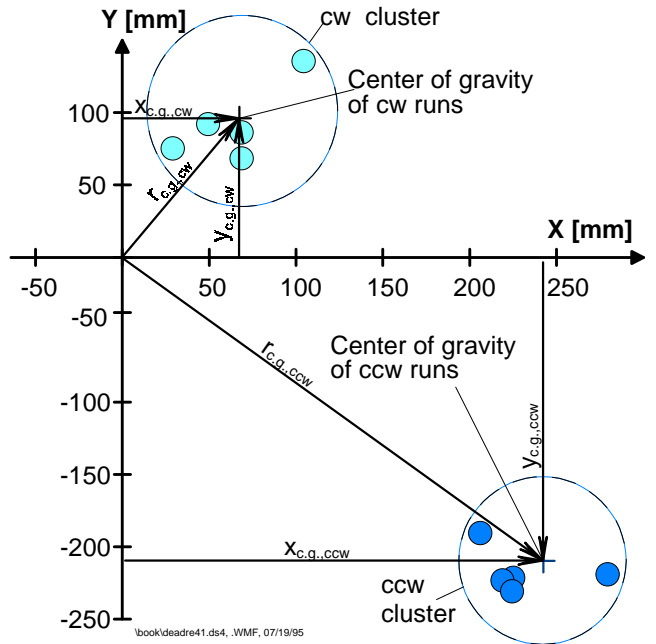


Figure 1: Typical results from running UMBmark (a square path run five times in cw and five times in ccw directions) with an uncalibrated TRC LabMate robot.

The results for many runs calibration sessions with TRC's LabMate robots averaged $E_{\max,\text{syst}} = 330$ mm for uncalibrated vehicles and $E_{\max,\text{syst}} = 24$ mm after calibration.

the UMBmark procedure, the *susceptibility* of a differential-drive platform to non-systematic errors can be expressed. Experimental results from six different vehicles, which were tested for their susceptibility to *non-systematic* error by means of the *extended UMBmark* test, are presented in Borenstein and Feng [1994].

Borenstein [1995] developed a method for detecting and rejecting non-systematic odometry errors in mobile robots. With this method, two collaborating platforms continuously and mutually correct their non-systematic (and certain systematic) odometry errors, even while both platforms are in motion. A video entitled “CLAPPER” showing this system in operation is included in [Borenstein et al., 1996b] and in [Borenstein 1995v]. A commercial version of this robot, shown in Figure 3, is now available from [TRC] under the name “*OmniMate*.” Because of its internal odometry error correction, the OmniMate is almost completely insensitive to bumps, cracks, or other irregularities on the floor [Borenstein, 1995; 1996].

2.2 Inertial Navigation

Inertial navigation uses gyroscopes and accelerometers to measure rate of rotation and acceleration, respectively. Measurements are integrated once (or twice, for accelerometers) to yield position. Inertial navigation systems have the advantage that they are self-contained, that is, they don't need external references. However, inertial sensor data drift with time because of the need to integrate rate data to yield position; any small constant error increases without bound after integration. Inertial sensors are thus mostly unsuitable for accurate positioning over an extended period of time.

2.2.1 Accelerometers

Test results from the use of accelerometers for mobile robot navigation have been generally poor. In an informal study at

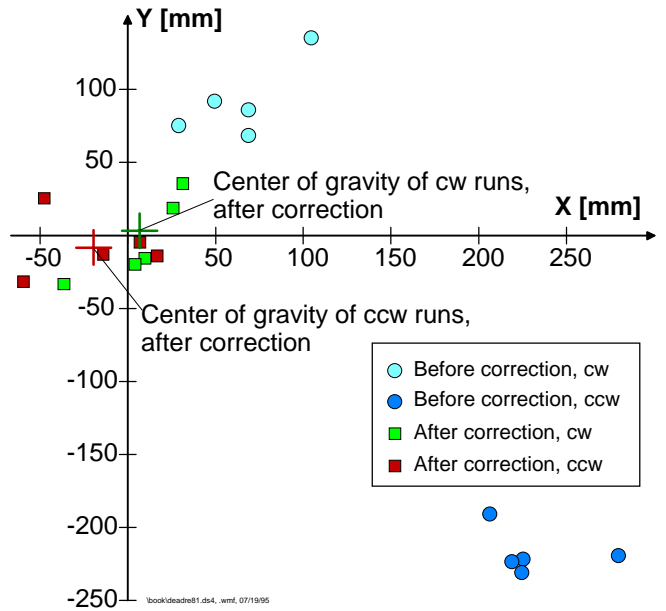


Figure 2: Position errors after completion of the bi-directional square-path experiment (4 x 4 m).



Figure 3: The OmniMate is a commercially available fully omnidirectional platform. The two linked “trucks” mutually correct their odometry errors.

the University of Michigan it was found that there is a very poor signal-to-noise ratio at lower accelerations (i.e., during low-speed turns). Accelerometers also suffer from extensive drift, and they are sensitive to uneven ground because any disturbance from a perfectly horizontal position will cause the sensor to detect a component of the gravitational acceleration g . One low-cost inertial navigation system aimed at overcoming the latter problem included a tilt sensor [Barshan and Durrant-Whyte, 1993; 1995]. The tilt information provided by the tilt sensor was supplied to the accelerometer to cancel the gravity component projecting on each axis of the accelerometer. Nonetheless, the results obtained from the tilt-compensated system indicate a position drift rate of 1 to 8 cm/s (0.4 to 3.1 in/s), depending on the frequency of acceleration changes. This is an unacceptable error rate for most mobile robot applications.

Table I: Selected specifications for the Andrew *Autogyro Navigator* (Courtesy of [Andrew Corp].)

Parameter	Value	Units
Input rotation rate	± 100	/s
Instantaneous bandwidth	100	Hz
Bias drift (at stabilized temperature) — RMS	0.005	/s rms
	18	/hr rms
Temperature range		
Operating	-40 to +75	°C
Storage	-50 to +85	°C
Warm up time	1	s
Size	115×90×41	mm
(excluding connector)	4.5×3.5×1.6	in
Weight (total)	0.25	kg
	0.55	lb
Power Analog	< 2	W
Power Digital	< 3	W

2.2.2 Gyroscopes

Gyroscopes (also known as “rate gyros” or just “gyros”) are of particular importance to mobile robot positioning because they can help compensate for the foremost weakness of odometry: in an odometry-based positioning method, any small momentary orientation error will cause a constantly growing lateral position error. For this reason it would be of great benefit if orientation errors could be detected and corrected immediately.

Until recently, highly accurate gyros were too expensive for mobile robot applications. For example, a high-quality inertial navigation system (INS) such as those found in a commercial airliner would have a typical drift of about 1850 meters (1 nautical mile) per hour of operation, and cost between \$50K and \$70K [Byrne et al., 1992]. High-end INS packages used in ground applications have shown performance of better than 0.1 percent of distance traveled, but cost in the neighborhood of \$100K to \$200K, while lower performance versions (i.e., one percent of distance traveled) run between \$20K to \$50K [Dahlin and Krantz, 1988].

However, very recently fiber-optic gyros (also called “laser gyros”), which are known to be very accurate, have fallen dramatically in price and have become a very attractive solution for mobile robot navigation.

One commercially available laser gyro is the “Autogyro Navigator” from Andrew Corp. [ANDREW], shown in Figure 4. It is a single-axis interferometric fiber-optic gyroscope (see [Everett, 1995] for technical details) based on polarization-maintaining fiber and precision fiber-

optic gyroscope technology. Technical specifications for Andrew's most recent model, the Auto-gyro *Navigator*, are shown in Table I. This laser gyro costs under \$1,000 and is well suited for mobile robot navigation.

2.3 Magnetic Compasses

Vehicle heading is the most significant of the navigation parameters (x , y , and θ) in terms of its influence on accumulated dead-reckoning errors. For this reason, sensors which provide a measure of absolute heading are extremely important in solving the navigation needs of autonomous platforms. The magnetic compass is such a sensor. One disadvantage of any magnetic compass, however, is that the earth's magnetic field is often distorted near power lines or steel structures [Byrne et al., 1992]. This makes the straightforward use of geomagnetic sensors difficult for indoor applications.

Based on a variety of physical effects related to the earth's magnetic field, different sensor systems are available:

- Mechanical magnetic compasses.
- Fluxgate compasses.
- Hall-effect compasses.
- Magnetoresistive compasses.
- Magnetoelastic compasses.

The compass best suited for use with mobile robot applications is the fluxgate compass. When maintained in a level attitude, the fluxgate compass will measure the horizontal component of the earth's magnetic field, with the decided advantages of low power consumption, no moving parts, intolerance to shock and vibration, rapid start-up, and relatively low cost. If the vehicle is expected to operate over uneven terrain, the sensor coil should be gimbal-mounted and mechanically damped to prevent serious errors introduced by the vertical component of the geomagnetic field.

Example: KVH Fluxgate Compasses

KVH Industries, Inc., Middletown, RI, offers a complete line of fluxgate compasses and related accessories, ranging from inexpensive units targeted for the individual consumer up through sophisticated systems intended for military applications [KVH]. The C100 COMPASS ENGINE shown in Figure 5 is a versatile, low-cost (less than \$700) developer's kit that includes a microprocessor-controlled stand-alone fluxgate sensor subsystem based on a two-axis toroidal ring-core sensor.

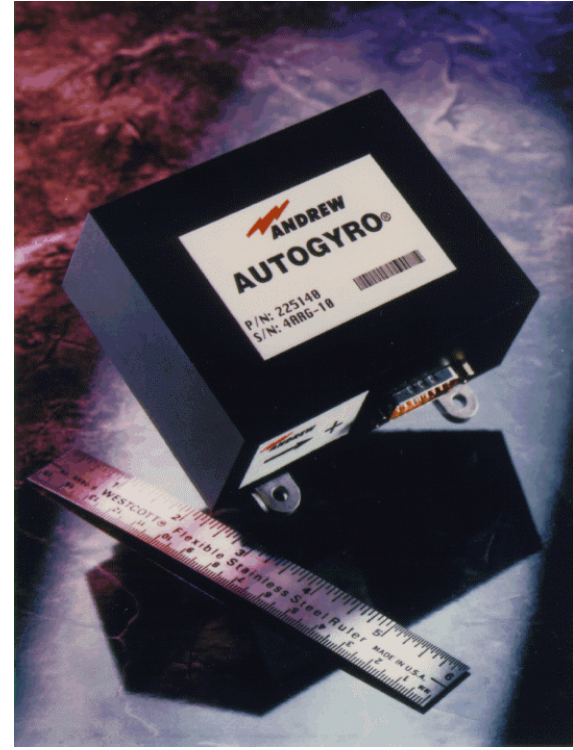


Figure 4: The Andrew AUTOGYRO Navigator. (Courtesy of [Andrew Corp].)

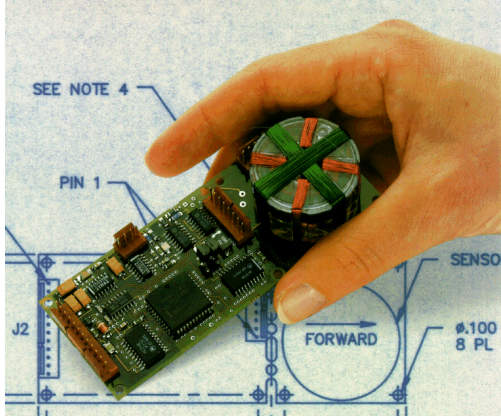


Figure 5: The C-100 fluxgate compass engine. (Courtesy of [KVH].)

Two different sensor options are offered with the C100: (1) The SE-25 sensor, recommended for applications with a tilt range of ± 16 degrees, and (2) the SE-10 sensor, for applications anticipating a tilt angle of up to ± 45 degrees.

The SE-25 sensor provides internal gimbaling by floating the sensor coil in an inert fluid inside the lexan housing. The SE-10 sensor provides a two-degree-of-freedom pendulous gimbal in addition to the internal fluid suspension. The SE-25 sensor mounts on top of the sensor PC board, while the SE-10 is suspended beneath it. The sensor PC board can be separated as much as 122 centimeters (48 in) from the detachable electronics PC board with an optional cable. Additional technical specifications are given in Table II.

2.4 Active Beacons

Active beacon navigation systems are the most common navigation aids on ships and airplanes, as well as on commercial mobile robot systems. Active beacons can be detected reliably and provide accurate positioning information with minimal processing. As a result, this approach allows high sampling rates and yields high reliability, but it does also incur high cost in installation and maintenance. Accurate mounting of beacons is required for accurate positioning. Two different types of active beacon systems can be distinguished: trilateration and triangulation.

2.4.1 Trilateration

Trilateration is the determination of a vehicle's position based on distance measurements to known beacon sources. In trilateration navigation systems there are usually three or more transmitters mounted at known locations in the environment and one receiver on board the robot. Conversely, there may be one transmitter on board and the receivers are mounted on the walls. Using time-of-flight information, the system computes the distance between the stationary transmitters and the onboard receiver. Global Positioning Systems (GPS), discussed in Section 2.5, are an example of trilateration.

Table II: Technical specifications for the KVH C-100 fluxgate compass. (Courtesy of [KVH]).

Parameter	Value	Units
Resolution	± 0.1	$^{\circ}$
Accuracy	± 0.5	$^{\circ}$
Repeatability	± 0.2	$^{\circ}$
Size	46×110	mm
	1.8×4.5	in
Weight (total)	62	gr
	2.25	oz
Power: Current drain	0.04	A
Supply voltage	8-18 or 18-28	V

2.4.2 Triangulation

In this configuration there are three or more active transmitters mounted at known locations, as shown in Figure 6. A rotating sensor on board the robot registers the angles λ_1 , λ_2 , and λ_3 at which it “sees” the transmitter beacons relative to the vehicle’s longitudinal axis. From these three measurements the unknown x- and y- coordinates and the unknown vehicle orientation can be computed. One problem with this configuration is that in order to be seen at distances of, say, 20 meters or more, the active beacons must be focused within a cone-shaped propagation pattern. As a result, beacons are not visible in many areas, a problem that is particularly grave because at least three beacons must be visible for triangulation.

Cohen and Koss [1992] performed a detailed analysis on three-point triangulation algorithms and ran computer simulations to verify the performance of different algorithms. The results are summarized as follows:

- The *Geometric Triangulation* method works consistently only when the robot is within the triangle formed by the three beacons. There are areas outside the beacon triangle where the geometric approach works, but these areas are difficult to determine and are highly dependent on how the angles are defined.
- The *Geometric Circle Intersection* method has large errors when the three beacons and the robot all lie on, or close to, the same circle.
- The *Newton-Raphson* method fails when the initial guess of the robot’s position and orientation is beyond a certain bound.
- The heading of at least two of the beacons was required to be greater than 90 degrees. The angular separation between any pair of beacons was required to be greater than 45 degrees.

In summary, it appears that none of the above methods alone is always suitable, but an intelligent combination of two or more methods helps overcome the individual weaknesses. .

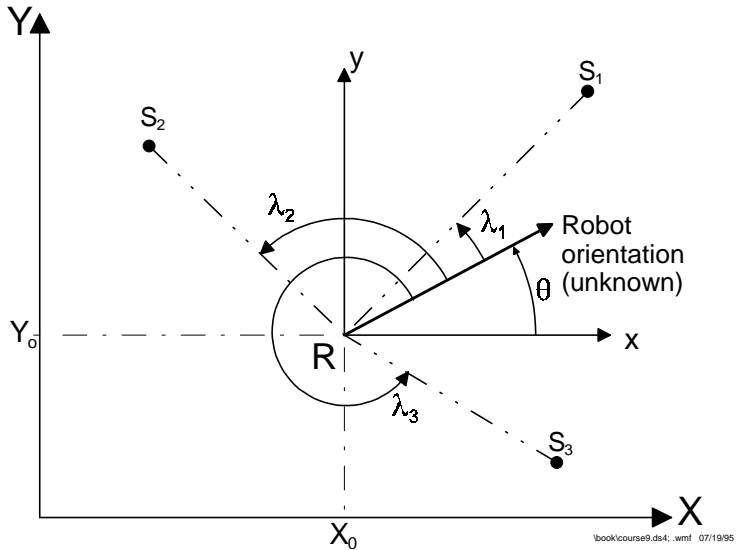


Figure 6: The basic triangulation problem: a rotating sensor head measures the three angles λ_1 , λ_2 , and λ_3 between the vehicle’s longitudinal axes and the three sources S_1 , S_2 , and S_3 .

ning mechanism operating in conjunction with fixed-location references strategically placed at predefined locations within the operating environment. A number of variations on this theme are seen in practice [Everett, 1995]: (a) scanning detectors with fixed active beacon emitters, (b) scanning emitter/detectors with passive retroreflective targets, (c) scanning emitter/detectors with active transponder targets, and (d) rotating emitters with fixed detector targets.

Example: MTI Research CONAC™

A similar type system using a predefined network of fixed-location detectors is made by MTI Research, Inc., Chelmsford, MA [MTI]. MTI's *Computerized Opto-electronic Navigation and Control* (CONAC™) is a navigational referencing system employing a vehicle-mounted laser unit called *STRuctured Opto-electronic Acquisition Beacon* (STROAB), as shown in Figure 7. The scanning laser beam is spread vertically to eliminate critical alignment, allowing the receivers, called *Networked Opto-electronic Acquisition Datums* (NOADs) (see Figure 8), to be mounted at arbitrary heights as illustrated in Figure 9. Detection of incident illumination by a NOAD triggers a response over the network to a host PC, which in turn calculates the implied

angles α_1 and α_2 . An index sensor built into the STROAB generates a rotation reference pulse to facilitate heading measurement. Indoor accuracy is on the order of centimeters or millimeters, and better than 0.1° for heading.

The reference NOADs are installed at known locations throughout the area of interest. STROAB acquisition range is sufficient to allow three NOADS to cover an area of $33,000 \text{ m}^2$ if no interfering structures block the view. Additional NOADS may be employed to increase fault tolerance and minimize ambiguities when two or more robots are operating in close proximity. The optimal set of three NOADS is dynamically selected by the host PC, based on the current location of the robot and any pre-defined visual barriers. A short video clip showing the CONAC system in operation is included in [Borenstein et al., 1996b]).



Figure 7: A single STROAB beams a vertically spread laser signal while rotating at 3,000 rpm. (Courtesy of MTI Research)



Figure 8: Stationary NOADs are located at known positions; at least two NOADs are networked and connected to a PC. (Courtesy of MTI Research, Inc.)

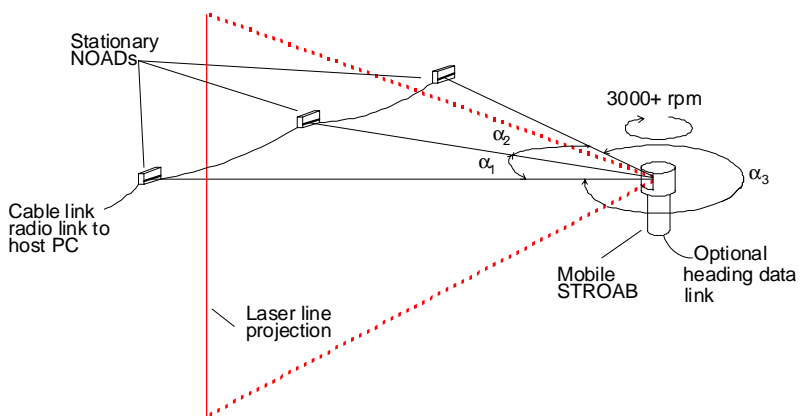


Figure 9: The CONAC™ system employs an onboard, rapidly rotating and vertically spread laser beam, which sequentially contacts the networked detectors. (Courtesy of MTI Research, Inc.)

2.5 Global Positioning Systems

The Global Positioning System (GPS) is a revolutionary technology for outdoor navigation. GPS was developed as a Joint Services Program by the Department of Defense. The system comprises 24 satellites (including three spares) which transmit encoded RF signals. Using advanced trilateration methods, ground-based receivers can compute their position by measuring the travel time of the satellites' RF signals, which include information about the satellites' momentary location. Knowing the exact distance from the ground receiver to three satellites theoretically allows for calculation of receiver latitude, longitude, and altitude.

The US government deliberately applies small errors in timing and satellite position to prevent a hostile nation from using GPS in support of precision weapons delivery. This intentional degradation in positional accuracy to around 100 meters (328 ft) worst case is termed selective availability (SA) [Gothard et al., 1993]. Selective availability has been on continuously (with a few exceptions) since the end of Operation Desert Storm. It was turned off during the war from August 1990 until July 1991 to improve the accuracy of commercial hand-held GPS receivers used by coalition ground forces. At another occasion (October 1992) SA was also turned off for a brief period while the Air Force was conducting tests. Byrne [1993] conducted tests at that time to compare the accuracy of GPS with SA turned on and off. The static measurements of the GPS error as a function of time (shown in Figure 10) were taken before the October 1992 test, i.e., with SA "on" (note the slowly varying error in Figure 10, which is caused by SA). By contrast, Figure 11 shows measurements from the October 1992 period when SA was briefly "off."

The effect of SA can be essentially eliminated through use of a practice known as differential GPS (DGPS). The concept is based on the premise that a second GPS receiver in fairly close proximity (i.e., within 10 km — 6.2 mi) to the first will experience basically the same error effects when viewing the same reference satellites. If this second receiver is fixed at a precisely surveyed location, its calculated solution can be compared to the known position to generate a composite error vector representative of prevailing conditions in that immediate locale. This differential correction can then be passed to the first receiver to null out the unwanted effects, effectively reducing position error for commercial systems.

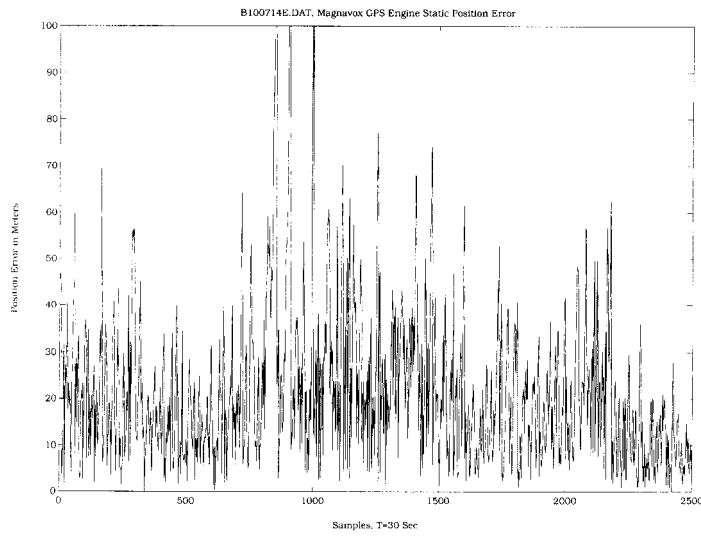
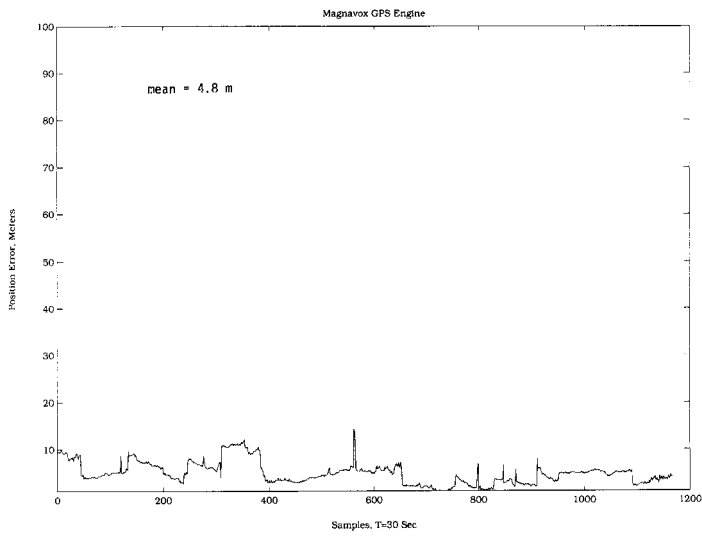


Figure 10: Typical GPS static position error with SA "On." (Courtesy of [Byrne, 1993].)

Many commercial GPS receivers are available with differential capability. This, together with the service of some local radio stations that make differential corrections available to subscribers of the service [GPS Report, 1992], makes the use of DGPS possible for many applications. Typical DGPS accuracies are around 4 to 6 meters (13 to 20 ft), with better performance seen as the distance between the mobile receivers and the fixed reference station is decreased. For example, the Coast Guard is in the process of implementing differential GPS in all major U.S. harbors, with an expected accuracy of around 1 meter (3.3 ft) [Getting, 1993]. A differential GPS system already in operation at O'Hare International Airport in Chicago has demonstrated that aircraft and service vehicles can be located to 1 meter (3.3 ft) in real-time, while moving. Surveyors use differential GPS to achieve centimeter accuracy, but this practice requires significant postprocessing of the collected data [Byrne, 1993].

Figure 11: Typical GPS static position error with SA "Off". (Courtesy of Byrne [1993]).



In 1992 and 1993 Raymond H. Byrne [1993] at the Advanced Vehicle Development Department, Sandia National Laboratories, Albuquerque, New Mexico conducted a series of in-depth comparison tests with five different GPS receivers. Testing focused on receiver sensitivity, static accuracy, dynamic accuracy, number of satellites tracked, and time-to-first-fix. The more important parameters evaluated in this test, the static and dynamic accuracy, are summarized below for the Magnavox GPS Engine, a representative of the five receivers tested.

Position Accuracy

Static position accuracy was measured by placing the GPS receivers at a surveyed location and taking data for approximately 24 hours. The plots of the static position error for the Magnavox GPS Engine was shown in Figure 10, above. The mean and standard deviation (σ) of the position error in this test was 22 meters (72 ft) and 16 meters (53 ft), respectively.

Fractional Availability of Signals

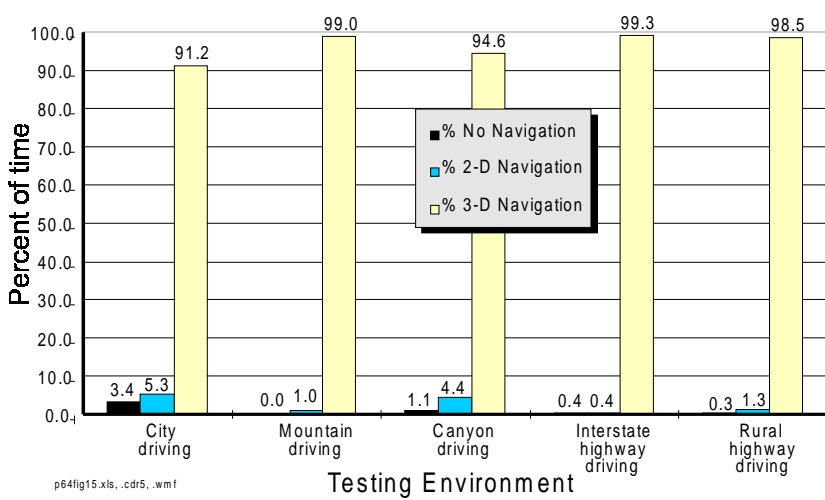
The dynamic test data was obtained by driving an instrumented van over different types of terrain. The various routes were chosen so that the GPS receivers would be subjected to a wide variety of obstructions. These include buildings, underpasses, signs, and foliage for the city driving. Rock cliffs and foliage were typical for the mountain and canyon driving. Large trucks, underpasses, highway signs, buildings, foliage, as well as small canyons were found on the interstate and rural highway driving routes.

The results of the dynamic testing are shown in Figure 12; the percentages have the following meaning:

No Navigation — Not enough satellites were in sight to permit positioning.

2-D Navigation — Enough satellites were in sight to determine the x- and y-coordinates of the vehicle.

3-D Navigation — Optimal Figure 12: Summary of dynamic environment performance for the data available. System could determine x-, y-, and z-coordinates of the vehicle.



In summary one can conclude that GPS is a tremendously powerful tool for many outdoor navigation tasks. The problems associated with using GPS for mobile robot navigation are: (a) periodic signal blockage due to foliage and hilly terrain, (b) multi-path interference, and (c) insufficient position accuracy for primary (stand-alone) navigation systems.

2.6 Landmark Navigation

Landmarks are distinct features that a robot can recognize from its sensory input. Landmarks can be geometric shapes (e.g., rectangles, lines, circles), and they may include additional information (e.g., in the form of bar-codes). In general, landmarks have a fixed and known position, relative to which a robot can localize itself. Landmarks are carefully chosen to be easy to identify; for example, there must be sufficient contrast relative to the background. Before a robot can use landmarks for navigation, the characteristics of the landmarks must be known and stored in the robot's memory. The main task in localization is then to recognize the landmarks reliably and to calculate the robot's position.

In order to simplify the problem of landmark acquisition it is often assumed that the current robot position and orientation are known approximately, so that the robot only needs to look for landmarks in a limited area. For this reason good odometry accuracy is a prerequisite for successful landmark detection.

Some approaches fall between landmark and map-based positioning (see Section 2.7). They use sensors to sense the environment and then extract distinct structures that serve as landmarks for navigation in the future.

Our discussion in this section addresses two types of landmarks: “artificial” and “natural” landmarks. It is important to bear in mind that “natural” landmarks work best in highly structured environments such as corridors, manufacturing floors, or hospitals. Indeed, one may argue that

“natural” landmarks work best when they are actually man-made (as is the case in highly structured environments). For this reason, we shall define the terms “natural landmarks” and “artificial landmarks” as follows: natural landmarks are those objects or features that are already in the environment and have a function other than robot navigation; artificial landmarks are specially designed objects or markers that need to be placed in the environment with the sole purpose of enabling robot navigation.

2.6.1 Natural Landmarks

The main problem in natural landmark navigation is to detect and match characteristic features from sensory inputs. The sensor of choice for this task is computer vision. Most computer vision-based natural landmarks are long vertical edges, such as doors, wall junctions, and ceiling lights (see TRC video clip in [Borenstein et al., 1996b]).

When range sensors are used for natural landmark navigation, distinct signatures, such as those of a corner or an edge, or of long straight walls, are good feature candidates. The selection of features is important since it will determine the complexity in feature description, detection, and matching. Proper selection of features will also reduce the chances for ambiguity and increase positioning accuracy.

Example: AECL's ARK Project

One system that uses natural landmarks was developed jointly by the Atomic Energy of Canada Ltd (AECL) and Ontario Hydro Technologies with support from the University of Toronto and York University [Jenkin et al., 1993]. This project aimed at developing a sophisticated robot system called the “*Autonomous Robot for a Known Environment*” (ARK).

The navigation module of the ARK robot is shown in Figure 13. The module consists of a custom-made pan-and-tilt table, a CCD camera, and an eye-safe IR spot laser rangefinder. Two VME-based cards, a single-board computer, and a microcontroller provide processing power. The navigation module is used to periodically correct the robot's accumulating odometry errors. The system uses natural landmarks such as alphanumeric signs, semi-permanent structures, or doorways. The only criteria used is that the landmark be distinguishable from the background scene by color or contrast.

The ARK navigation module uses an interesting hybrid approach: the system stores (learns) landmarks by generating a three-dimensional “gray-level surface” from a single training image

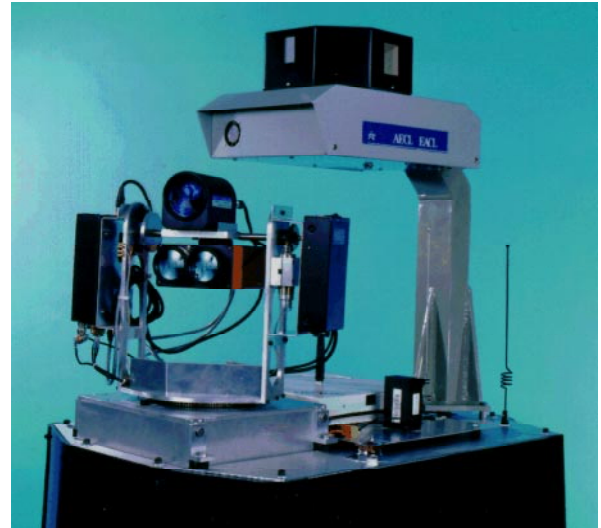


Figure 13: The ARK's natural landmark navigation system uses a CCD camera and a time-of-flight laser rangefinder to identify landmarks and to measure the distance between landmark and robot. (Courtesy of Atomic Energy of Canada Ltd.)

obtained from the CCD camera. A coarse, registered range scan of the same field of view is performed by the laser rangefinder, giving depths for each pixel in the gray-level surface. Both procedures are performed from a known robot position. Later, during operation, when the robot is at an approximately known (from odometry) position within a couple of meters from the training position, the vision system searches for those landmarks that are expected to be visible from the robot's momentary position. Once a suitable landmark is found, the projected appearance of the landmark is computed. This expected appearance is then used in a coarse-to-fine normalized correlation-based matching algorithm that yields the robot's relative distance and bearing with regard to that landmark. With this procedure the ARK can identify different natural landmarks and measure its position relative to the landmarks. A video clip showing the ARK system in operation is included in [Borenstein et al., 1996b]).

2.6.2 Artificial Landmarks

Detection is much easier with artificial landmarks [Atiya and Hager, 1993], which are designed for optimal contrast. In addition, the exact size and shape of artificial landmarks are known in advance. Size and shape can yield a wealth of geometric information when transformed under the perspective projection.

Researchers have used different kinds of patterns or marks, and the geometry of the method and the associated techniques for position estimation vary accordingly [Talluri and Aggarwal, 1993]. Many artificial landmark positioning systems are based on computer vision. We will not discuss these systems in detail, but will mention some of the typical landmarks used with computer vision. Fukui [1981] used a diamond-shaped landmark and applied a least-squares method to find line segments in the image plane. Other systems use reflective material patterns and strobed light to ease the segmentation and parameter extraction [Lapin, 1992; Mesaki and Masuda, 1992]. There are also systems that use active (i.e., LED) patterns to achieve the same effect [Fleury and Baron, 1992].

The accuracy achieved by the above methods depends on the accuracy with which the geometric parameters of the landmark images are extracted from the image plane, which in turn depends on the relative position and angle between the robot and the landmark. In general, the accuracy decreases with the increase in relative distance. Normally there is a range of relative angles in which good accuracy can be achieved, while accuracy drops significantly once the relative angle moves out of the “good” region.

There is also a variety of landmarks used in conjunction with non-vision sensors. Most often used are bar-coded reflectors for laser scanners. For example, work on the *Mobile Detection Assessment and Response System* (MDARS) [Everett et al., 1994; DeCorte, 1994; Everett 1995] uses retro-reflectors, and so does the commercially available system from Caterpillar on their *Self-Guided Vehicle* [Gould, 1990; Byrne et al., 1992]. The shape of these landmarks is usually unimportant. By contrast, a unique approach taken by Feng et al. [1992] used a circular landmark and applied an optical Hough transform to extract the parameters of the ellipse on the image plane in real time.

We summarize the characteristics of landmark-based navigation as follows:

- Natural landmarks offer flexibility and require no modifications to the environment.
- Artificial landmarks are inexpensive and can have additional information encoded as patterns or shapes.
- The maximal effective distance between robot and landmark is substantially shorter than in active beacon systems.
- The positioning accuracy depends on the distance and angle between the robot and the landmark. Landmark navigation is rather inaccurate when the robot is further away from the landmark. A higher degree of accuracy is obtained only when the robot is near a landmark.
- Substantially more processing is necessary than with active beacon systems. In many cases onboard computers cannot process natural landmark algorithms quickly enough for real-time motion.
- Ambient conditions, such as lighting, can be problematic; in marginal visibility landmarks may not be recognized at all or other objects in the environment with similar features can be mistaken for a legitimate landmark. This is a serious problem because it may result in a completely erroneous determination of the robot's position.
- Landmarks must be available in the work environment around the robot.
- Landmark-based navigation requires an approximate starting location so that the robot knows where to look for landmarks. If the starting position is not known, the robot has to conduct a time-consuming search process. This search process may go wrong and may yield an erroneous interpretation of the objects in the scene.
- A database of landmarks and their location in the environment must be maintained.
- There is only limited commercial support for natural landmark-based techniques.

2.7 Map-based Positioning

Map-based positioning, also known as “map matching,” is a technique in which the robot uses its sensors to create a map of its local environment. This local map is then compared to a global map previously stored in memory. If a match is found, then the robot can compute its actual position and orientation in the environment. The pre-stored map can be a CAD model of the environment, or it can be constructed from prior sensor data. Map-based positioning is advantageous because it uses the naturally occurring structure of typical indoor environments to derive position information without modifying the environment. Also, with some of the algorithms being developed, map-based positioning allows a robot to learn a new environment and to improve positioning accuracy through exploration. Disadvantages of map-based positioning are the stringent requirements for accuracy of the sensor map, and the requirement that there be enough stationary, easily distinguishable features that can be used for matching. Because of the challenging requirements currently most work in map-based positioning is limited to laboratory settings and to relatively simple environments.

2.7.1 Map Building

There are two fundamentally different starting points for the map-based positioning process. Either there is a pre-existing map, or the robot has to build its own environment map. Rencken

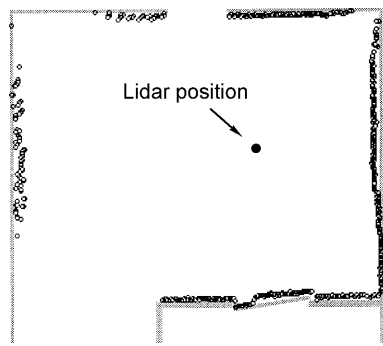


Figure 14: A typical scan of a room, produced by the University of Kaiserslautern's in-house developed lidar system. (Courtesy of the University of Kaiserslautern.)

[1993] defined the map building problem as the following: “Given the robot's position and a set of measurements, what are the sensors seeing?” Obviously, the map-building ability of a robot is closely related to its sensing capacity.

A problem related to map-building is “autonomous exploration” [Rencken, 1994]. In order to build a map, the robot must explore its environment to map uncharted areas. Typically it is assumed that the robot begins its exploration without having any knowledge of the environment. Then, a certain motion strategy is followed which aims at maximizing the amount of charted area in the least amount of time. Such a motion strategy is called “exploration strategy,” and it depends strongly on the kind of sensors used. One example for a simple exploration strategy based on a lidar sensor is given by [Edlinger and Puttkamer, 1994].

Many researchers believe that no single sensor modality alone can adequately capture all relevant features of a real environment. To overcome this problem, it is necessary to combine data from different sensor modalities, a process known as sensor fusion. For example, Buchberger et al. [1993] and Jörg [1994; 1995] developed a mechanism that utilizes heterogeneous information obtained from a laser-radar and a sonar system in order to construct reliable and complete world models. Sensor fusion is an active research area, and the literature is replete with techniques that combine various types of sensor data.

2.7.2 Map Matching

One of the most important and challenging aspects of map-based navigation is map matching, i.e., establishing the correspondence between a current local map and a stored global map [Kak et al., 1990]. Work on map matching in the computer vision community is often focused on the general problem of matching an image of arbitrary position and orientation relative to a model (e.g., [Talluri and Aggarwal, 1993]). In general, matching is achieved by first extracting features, followed by determination of the correct correspondence between image and model features, usually by some form of constrained search [Cox, 1991]. A discussion of two different classes of matching algorithms, “icon-based” and “feature-based,” are given in [Schaffer et al., 1992].

Example: University of Kaiserslautern's Angle Histogram

A simple but apparently very effective method for map-building was developed by Hinkel and Knieriemen [1988] from the University of Kaiserslautern, Germany. This method, called the “Angle Histogram,” used an in-house developed lidar. A typical scan from this lidar is shown in Figure 14.

The angle histogram method works as follows. First, a 360-degree scan of the room is taken with the lidar, and the resulting “hits” are recorded in a map. Then the algorithm measures the relative angle δ between any two adjacent hits (see Figure 15). After compensating for noise in

the readings (caused by the inaccuracies in position between adjacent hits), the angle histogram shown in Figure 16(a) can be built. The uniform direction of the main walls are clearly visible as peaks in the angle histogram. Computing the histogram modulo π results in only two main peaks: one for each pair of parallel walls. This algorithm is very robust with regard to openings in the walls, such as doors and windows, or even cabinets lining the walls.

After computing the angle histogram, all angles of the hits can be normalized, resulting in the representation shown in Figure 16b. After this transformation, two additional histograms, one for the x- and one for the y-direction can be constructed. This time, peaks show the distance to the walls in x and y direction. Hinkel and Knieriem's original algorithms have been further refined over the past years (e.g., Weiß et al. [1994]) and the Angle Histogram method is now said to yield a reliable accuracy of 0.5° .

Example 2: Siemens' Roamer

Rencken [1993; 1994] at the Siemens Corporate Research and Development Center in Munich, Germany, has made substantial contributions toward solving the boot strap problem resulting from the uncertainty in position and environment. This problem exists when a robot must move around in an unknown environment, with uncertainty in its odometry-derived position. For

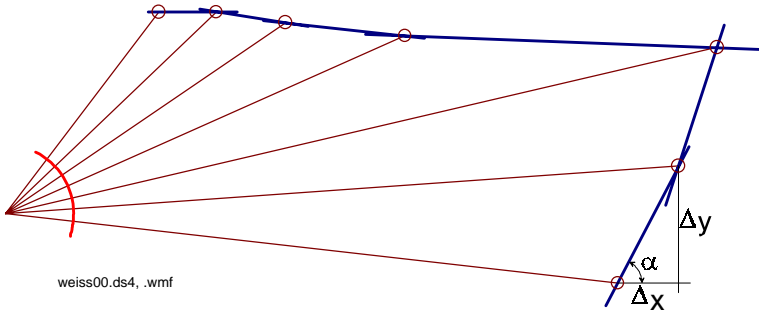


Figure 15: Calculating angles for the angle histogram.
(Courtesy of [Weiß et al., 1994].)

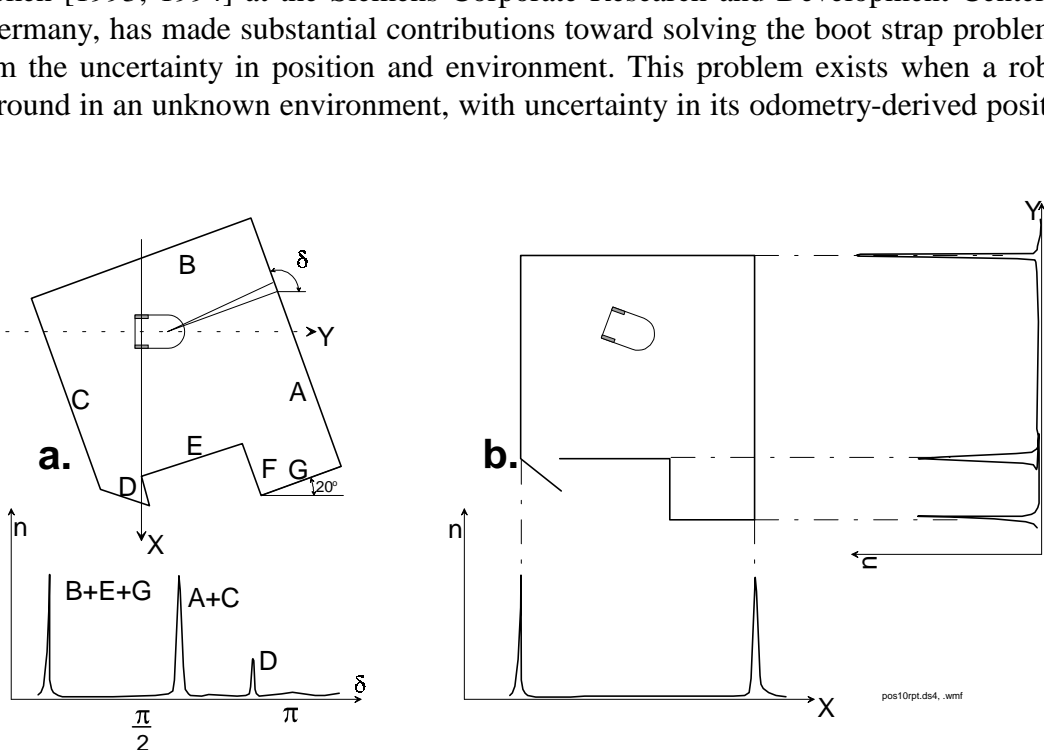


Figure 16: Readings from a rotating laser scanner generate the contours of a room.

- The angle histogram allows the robot to determine its orientation relative to the walls.
- After normalizing the orientation of the room relative to the robot, an x-y histogram can be built from the same data points. (Adapted from [Hinkel and Knieriem, 1988].)

example, when building a map of the environment, all measurements are necessarily relative to the carrier of the sensors (i.e., the mobile robot). Yet, the position of the robot itself is not known exactly, because of the errors accumulating in odometry.

Rencken addresses the problem as follows: in order to represent features “seen” by its 24 ultrasonic sensors, the robot constructs hypotheses about these features. To account for the typically unreliable information from ultrasonic sensors, features can be classified as hypothetical, tentative, or confirmed. Once a feature is confirmed, it is used for constructing the map. Before the map can be updated, though, every new data point must be associated with either a plane, a corner, or an edge (and some variations of these features). Rencken devises a “hypothesis tree” which is a data structure that allows tracking of different hypotheses until a sufficient amount of data has been accumulated to make a final decision.

3. CONCLUSIONS

This paper presented an overview over existing sensors and techniques for mobile robot positioning. We defined seven categories for these sensors and techniques, but obviously other ways for organizing the subject are possible. The foremost conclusion we could draw from reviewing the vast body of literature was that for indoor mobile robot navigation no single, elegant solution exists. For outdoor navigation GPS is promising to become the universal navigation solution for almost all automated vehicle systems.

Unfortunately, an indoor equivalent to GPS is difficult to realize because none of the currently existing RF-based trilateration systems work reliably indoors. If line-of sight between stationary and onboard components can be maintained, then RF-based solutions can work indoors as well. However, in that case optical components using triangulation are usually less expensive. The market seems to have adopted this thought some time ago, as can be seen in the relatively large number of commercially available navigation systems that are based on optical triangulation (as discussed in Section 2.4.3).

Despite the variety of powerful existing systems and techniques, we believe that mobile robotics is still in need for a particularly elegant and universal indoor navigation method. Such a method will likely bring scientific recognition and commercial success to its inventor.

Appendix A: Tabular comparison of Positioning Systems

System & Description	Features	Accuracy – Position [mm]	Accuracy – orientation [°]	Effective Range	Reference
Odometry on TRC LabMate, after UMBmark calibration. Wheel-encoder resolution: 0.012 mm linear travel per pulse	4×4 meters square path: smooth floor: 30 mm, 10 bumps: 500 mm	Smooth floor: 1-2°. With 10 bumps: 8°	Unlimited	[Borenstein and Feng, 1995]	
CLAPPER and OmniMate: Dual-drive robot with internal correction of odometry. Made from two TRC LabMates, connected by compliant linkage. Uses 2 abs. rotary encoders, 1 linear encoder.	4×4 m square path: smooth floor: ~20 mm 10 bumps: ~40 mm	smooth floor: <1° 10 bumps: <1°	Unlimited	[Borenstein, 1995; 1996]	
Complete inertial navigation system including ENV-O5S Gyrostar solid state rate gyro, START solid state gyro, triaxial linear accelerometer and 2 inclinometers	Position drift rate: 1-8 cm/s depending on frequency of acceleration change	Drift: 5-0.25°/s. After compensation drift 0.0125°/s	Unlimited	[Barshan and Durrant-Whyte, 1993; 1995]	
Andrew Autogyro and Autogyro Navigator. Quoted minimum detectable rotation rate: $\pm 0.02^{\circ}/s$. Actual minimum detectable rate limited by deadband after A/D conversion: 0.0625°/s. Cost: \$1000	Not applicable	Drift: 0.005°/s	Unlimited	[ANDREW]	
KVH Fluxgate Compass. Includes microprocessor-controlled fluxgate sensor subsystem. Cost <\$700	Not applicable	Resolution: $\pm 0.5^{\circ}$ Accuracy: $\pm 0.5^{\circ}$ Repeatability: $\pm 0.2^{\circ}$	Unlimited	[KVH]	
CONAC™ (computerized opto-electronic navigation and control). Cost: \$6,000.	Measures both angle and distance to target	Indoor ± 1.3 mm outdoor ± 5 mm	Indoor and outdoor $\pm 0.05^{\circ}$	> 100 m	[McLeod, 1993]; [MTI]
Global Positioning Systems (GPS). Cost: \$1,000 - \$5,000.		order of 20 m during motion, order of centimeters when standing for minutes	Not applicable	Unlimited	Different vendors
Landmark Navigation		<5 cm	< 1 deg	~10 m	Different research projects
Model Matching (map-based positioning)		order of 1-10 cm	order of 1-3 deg	~10 m	Different research projects

Acknowledgment:

Parts of this research was funded by Department of Energy Grant DE-FG02-86NE37969. Parts of the text were adapted from [Borenstein et al., 1996; Everett, 1995; Byrne, 1993].

4. REFERENCES

1. Atiya, S. and Hager, G., 1993, "Real-time Vision-based Robot Localization." *IEEE Transactions on Robotics and Automation*, Vol. 9, No. 6, pp. 785-800.
2. Barshan, B. and Durrant-Whyte, H.F., 1993, "An Inertial Navigation System for a Mobile Robot." *Proceedings of the 1993 IEEE/RSJ International Conference on Intelligent Robotics and Systems*, Yokohama, Japan, July 26-30, pp. 2243-2248.
3. Barshan, B. and Durrant-Whyte, H.F., 1995, "Inertial Navigation Systems Mobile Robots." *IEEE Transactions on Robotics and Automation*, Vol. 11, No. 3, June, pp. 328-342.
4. Battin, R. H., 1987, "An Introduction to the Mathematics and Methods of Astrodynamics." AIAA Education Series, New York, NY, ISBN 0-930403-25-8.
5. Borenstein, J. and Feng, L., 1994, "UMBmark — A Method for Measuring, Comparing, and Correcting Dead-reckoning Errors in Mobile Robots." *Technical Report, The University of Michigan UM-MEAM-94-22*, December.
6. Borenstein, J., 1995, "Internal Correction of Dead-reckoning Errors With the Compliant Linkage Vehicle." *Journal of Robotic Systems*, Vol. 12, No. 4, April 1995, pp. 257-273.
7. Borenstein, J., 1995v, "The CLAPPER: A Dual-drive Mobile Robot With Internal Correction of Dead-reckoning Errors." *Video Proceedings of the 1995 IEEE International Conference on Robotics and Automation*, Nagoya, Japan, May 21-27, 1995.
8. Borenstein, J. and Feng. L., 1995, "UMBmark: A Benchmark Test for Measuring Dead-reckoning Errors in Mobile Robots." *1995 SPIE Conference on Mobile Robots*, Philadelphia, October 22-26.
9. Borenstein, J. and Feng. L., 1996, "Measurement and Correction of Systematic Odometry Errors in Mobile Robots." *IEEE Journal of Robotics and Automation*, Vol 12, No 5, October.
10. Borenstein, J., Everett, B., and Feng, L., 1996a, "Navigating Mobile Robots: Systems and Techniques." A. K. Peters, Ltd., Wellesley, MA, ISBN 1-56881-058-X.
11. Borenstein, J., Everett, B., and Feng, L., 1996b, "Navigating Mobile Robots: Systems and Techniques." *CD-ROM Edition*, A. K. Peters, Ltd., Wellesley, MA, ISBN 1-56881-058-X.
12. Borenstein, J., 1996, "Experimental Results from Internal Odometry Error Correction With the OmniMate Mobile Platform." Submitted to *the IEEE Transactions on Robotics and Automation*, July 1996.
13. Buchberger, M., Jörg, K., and Puttkamer, E., 1993, "Laserradar and Sonar Based World Modeling and Motion Control for Fast Obstacle Avoidance of the Autonomous Mobile Robot MOBOT-IV." *Proceedings of IEEE International Conference on Robotics and Automation*, Atlanta, GA, May 10-15, pp. 534-540.
14. Byrne, R.H., Klarer, P.R., and Pletta, J.B., 1992, "Techniques for Autonomous Navigation." *Sandia Report SAND92-0457*, Sandia National Laboratories, Albuquerque, NM, March.
15. Byrne, R.H., 1993, "Global Positioning System Receiver Evaluation Results." *Sandia Report SAND93-0827*, Sandia National Laboratories, Albuquerque, NM, Sept.

16. Chenavier, F. and Crowley, J., 1992, "Position Estimation for a Mobile Robot Using Vision and Odometry." *Proceedings of IEEE International Conference on Robotics and Automation*, Nice, France, May 12-14, pp. 2588-2593.
17. Cohen, C. and Koss, F., 1992, "A Comprehensive Study of Three Object Triangulation." *Proceedings of the 1993 SPIE Conference on Mobile Robots*, Boston, MA, Nov. 18-20, pp. 95-106.
18. Cox, I.J., 1991, "Blanche - An Experiment in Guidance and Navigation of an Autonomous Mobile Robot." *IEEE Transactions Robotics and Automation*, 7(3), pp. 193-204.
19. Dahlin, T. and Krantz, D., 1988, "Low-Cost, Medium-Accuracy Land Navigation System." *Sensors*, Feb., pp. 26-34.
20. DeCorte, C., 1994, "Robots Train for Security Surveillance." *Access Control*, June, pp. 37-38.
21. Edlinger, T. and Puttkamer, E., 1994, "Exploration of an Indoor Environment by an Autonomous Mobile Robot." *International Conference on Intelligent Robots and Systems (IROS '94)*. Munich, Germany, Sept. 12-16, pp. 1278-1284.
22. Everett, H.R., Gage, D.W., Gilbreth, G.A., Laird, R.T., and Smurlo, R.P., 1994, "Real-World Issues in Warehouse Navigation." *Proceedings SPIE Mobile Robots IX*, Volume 2352, Boston, MA, Nov. 2-4.
23. Everett, H. R., 1995, *Sensors for Mobile Robots: Theory and Application*, A K Peters, Ltd., Wellesley, MA, ISBN 1-56881-048-2.
24. Farrell, J. L., 1976, "Integrated Aircraft Navigation." Academic Press, New York, NY, ISBN 0-12-249750-3.
25. Feng, L., Fainman, Y., and Koren, Y., 1992, "Estimate of Absolute Position of Mobile Systems by Opto-electronic Processor," *IEEE Transactions on Man, Machine and Cybernetics*, Vol. 22, No. 5, pp. 954-963.
26. Fleury, S. and Baron, T., 1992, "Absolute External Mobile Robot Localization Using a Single Image." *Proceedings of the 1992 SPIE Conference on Mobile Robots*, Boston, MA, Nov. 18-20, pp. 131-143.
27. Fukui, I., 1981, "TV Image Processing to Determine the Position of a Robot Vehicle." *Pattern Recognition*, Vol. 14, pp. 101-109.
28. Getting, I.A., 1993, "The Global Positioning System," *IEE Spectrum*, December, pp. 36-47.
29. Gothard, B.M., Etersky, R.D., and Ewing, R.E., 1993, "Lessons Learned on a Low-Cost Global Navigation System for the Surrogate Semi-Autonomous Vehicle." *SPIE Proceedings*, Vol. 2058, Mobile Robots VIII, pp. 258-269.
30. Gould, L., 1990, "Is Off-Wire Guidance Alive or Dead?" *Managing Automation*, May, pp. 38-40.
31. *GPS Report*. November 5, 1992. Potomac, MD: Phillips Business Information.
32. Hinkel, R. and Knieriemen, T., 1988, "Environment Perception with a Laser Radar in a Fast Moving Robot." *Symposium on Robot Control 1988 (SYROCO '88)*, Karlsruhe, Germany, October 5-7, pp. 68.1 - 68.7.
33. Jenkin, M., Milius, E., Jasiobedzki, P., Bains, N., and Tran, K., 1993, "Global Navigation for ARK." *Proceedings of the 1993 IEEE/RSJ International Conference on Intelligent Robotics and Systems*, Yokohama, Japan, July 26-30, pp. 2165-2171.

34. Jörg, K.W., 1994, "Echtzeitfähige Multisensorintegration für autonome mobile Roboter." ISBN 3-411-16951-6, B.I. Wissenschaftsverlag, Mannheim, Leipzig, Wien, Zürich.
35. Jörg, K.W., 1995, "World Modeling for an Autonomous Mobile Robot Using Heterogenous Sensor Information." *Robotics and Autonomous Systems*, Vol. 14, pp. 159-170.
36. Kak, A., Andress, K., Lopez-Abadia, and Carroll, M., 1990, "Hierarchical Evidence Accumulation in the PSEIKI System and Experiments in Model-driven Mobile Robot Navigation." *Uncertainty in Artificial Intelligence*, Vol. 5, Elsevier Science Publishers B. V., North-Holland, pp. 353-369.
37. Lapin, B., 1992, "Adaptive Position Estimation for an Automated Guided Vehicle." *Proc. of the 1992 SPIE Conference on Mobile Robots*, Boston, MA, Nov. 18-20, pp. 82-94.
38. Mesaki, Y. and Masuda, I., 1992, "A New Mobile Robot Guidance System Using Optical Reflectors." *Proceedings of the 1992 IEEE/RSJ International Conference on Intelligent Robots and Systems*, Raleigh, NC, July 7-10, pp. 628-635.
39. Rencken, W.D., 1993, "Concurrent Localization and Map Building for Mobile Robots Using Ultrasonic Sensors." *Proceedings of the 1993 IEEE/RSJ International Conference on Intelligent Robotics and Systems*, Yokohama, Japan, July 26-30, pp. 2192-2197.
40. Rencken, W.D., 1994, "Autonomous Sonar Navigation in Indoor, Unknown, and Unstructured Environments." *1994 International Conference on Intelligent Robots and Systems (IROS '94)*, Munich, Germany, Sept. 12-16, pp. 127-134.
41. Talluri, R., and Aggarwal, J., 1993, "Position Estimation Techniques for an Autonomous Mobile Robot - a Review." in *Handbook of Pattern Recognition and Computer Vision*, World Scientific: Singapore, Chapter 4.4, pp. 769-801.
42. Weiβ, G., Wetzler, C., and Puttkamer, E., 1994, "Keeping Track of Position and Orientation of Moving Indoor Systems by Correlation of Range-Finder Scans." *1994 International Conference on Intelligent Robots and Systems (IROS '94)*, Munich, Germany, Sept. 12-16, pp. 595-601.

Commercial Companies

43. ANDREW Andrew Corporation, 10500 W. 153rd Street, Orland Park, IL 60462. 708-349-5294 or 708-349-3300.
44. DBIR - Denning Branch International Robotics, 1401 Ridge Avenue, Pittsburgh PA 15233, 412-322-4412.
45. KVH - KVH Industries, C100 Compass Engine Product Literature, 110 Enterprise Center, Middletown, RI 02840, 401-847-3327.
46. MTI - MTI Research, Inc., 313 Littleton Road, Chelmsford, MA 01824., 508-250-4949.
47. TRC - Transitions Research Corp. (now under new name: "HelpMate Robotics Inc. – HRI"), Shelter Rock Lane, Danbury, CT 06810, 203-798-8988.